AD-A062 437 AERONAUTICAL RESEARCH LABS MELBOURNE (AUSTRALIA) F/G 11/6
ON THE STRESS ANALYSIS OF PATCHED CRACKS.(U)
JAN 78 R JONES, R J CALLINAN

UNCLASSIFIED ARL/STRUC-367 NL

| OF |
AD
A062437

END
DATE
FILMED
3-79
DDC

ARL-Struc-Report-367

LEVEL II

AR-000-1113

DEPARTMENT OF DEFENCE

DEFENCE SCIENCE AND TECHNOLOGY ORGANISATION

AERONAUTICAL RESEARCH LABORATORIES

MELBOURNE, VICTORIA

STRUCTURES REPORT 367

ON THE STRESS ANALYSIS OF PATCHED CRACKS

by

R. JONES and R. J. CALLINAN

Approved For Public Release.

COPY No 7

January, 1978

LEVEL II

AR-000-1113

DEPARTMENT OF DEFENCE
DEFENCE SCIENCE AND TECHNOLOGY ORGANISATION
AERONAUTICAL RESEARCH LABORATORIES

(11) Jan 78

(9) STRUCTURES REPORT, 367

(6) ON THE STRESS ANALYSIS OF PATCHED CRACKS

by

R. JONES and R. J. CALLINAN

(10) Rhys/Jones Richard J./Callinan

(14) ARL/STRUC-367 (12) 37 p.

SUMMARY

A finite element method for analysing the behaviour of cracks in metal sheets, which are patched with an overlay of composite material, is described. The analysis includes the separate responses of the sheet, composite patch and the adhesive. Debonding of the adhesive is permitted and the stress intensity factor at the crack tip is obtained as well as the stress distribution in the patch.

POSTAL ADDRESS: Chief Superintendent, Aeronautical Research Laboratories,
Box 4331, P.O., Melbourne, Victoria, 3001, Australia.

DOCUMENT CONTROL DATA SHEET

Security classification of this page: UNCLASSIFIED

1. Document Numbers (a) AR Number: AR-000-1113 (b) Document Series and Number: Structures Report 367 (c) Report Number: ARL—Struc—Report—368 ✓	2. Security Classification (a) Complete document: Unclassified (b) Title in isolation: Unclassified (c) Summary in isolation: Unclassified

3. Title: ON THE STRESS ANALYSIS OF PATCHED CRACKS

4. Personal Author(s): Jones, Rhys Callinan, Richard J.	5. Document Date: January, 1978 6. Type of Report and Period Covered:
7. Corporate Author(s): Aeronautical Research Laboratories 9. Cost Code: 21 4670	8. Reference Numbers (a) Task: AIR 72/20 (b) Sponsoring Agency: Department of Defence (Air)
10. Imprint: Aeronautical Research Laboratories ✓	11. Computer Program(s) (Title(s) and language(s)):

12. Release Limitations (of the document): Approved for Public Release

12-0. Overseas:	No.		P.R.	1	A		B		C		D		E	

13. Announcement Limitations (of the information on this page):
No Limitation

14. Descriptors:		15. Cosati Codes:
Metal sheets	Maintenance	1113
Cracking (Fracturing)	Stress analysis	2012
Cracks	Finite element method	1402
Composite materials		

16. *ABSTRACT*

A finite element method for analysing the behaviour of cracks in metal sheets, which are patched with an overlay of composite material, is described. The analysis includes the separate responses of the sheet, composite patch and the adhesive. Debonding of the adhesive is permitted and the stress intensity factor at the crack tip is obtained as well as the stress distribution in the patch.

CONTENTS

NOTATION

σ_x, σ_y	Direct stresses in the patch.
τ_{xz}, τ_{yz}	Transverse shear stresses.
$\underset{\sim}{\lambda}$	Elemental displacement vector.
θ	Angle measured from local axis system to the material symmetry axis.
$\phi_i(x, y)$	Distribution function of the transverse shear stresses within an element of the adhesive.
γ_{xz}, γ_{yz}	Transverse shear strains.
ϵ_x, ϵ_y	Strains in the patch.
x, y, z	In-plane coordinates and the coordinate in the thickness direction respectively.
t_s, t_a, t_o	Thicknesses of the sheet, adhesive, and patch respectively.
ν_s	Poisson's ratio for the sheet.
G_s, G_a	Shear moduli of the sheet and adhesive respectively.
G_{13}, G_{23}	Transverse shear moduli of the patch in the xz and yz planes respectively.
u_o, v_o	Displacements at the mid surface of the patch.
u_s, v_s	Displacements at the mid surface of the sheet.
V_a	Strain energy of the adhesive.
K_1	Mode 1 stress intensity factor.
$K^e{}_a$	Element stiffness matrix for the adhesive.
$K^e{}_p$	Element stiffness matrix for the patch.
K^e	Element stiffness matrix for the adhesive-patch pair.

1. INTRODUCTION

A bonded overlay of high strength composite material offers an efficient method for reducing the stress intensity factor, and hence the stress field at the tip of a crack. This reduction in the stress intensity factor subsequently retards crack growth. The primary objective of the work reported here is to develop a method of analysis for a crack which has been patched. The development is based upon the finite element method for analysing cracked structures as previously described[1,2] by the authors. The present analysis is an extension of this previous work to patched cracks, and it allows for separate responses of the adhesive and the composite patch as well as the debonding of the patch from the sheet.

This report forms the first section of a detailed investigation into crack patching and, as indicated above, its main purpose is to develop the theoretical tools for the investigation. A detailed study into the effects of changing the geometry of the patch as well as changing its material properties is to be reported in a subsequent paper.

2. METHOD OF ANALYSIS

Let us begin by considering a thin composite patch which is bonded to a thin elastic sheet. The x and y axes are taken in a plane parallel to the mid-surface of the sheet while the z-axis is in the thickness direction. The sheet is subsequently acted upon by a system of external loads acting at its edges and with lines of action lying in its plane. When the patch is not present this problem is usually tackled under the assumptions of generalized plane stress. However, when the patch is present shear stresses will be developed in the adhesive bond and it is reasonable to assume that these will be continuous across the adhesive-sheet interface as well as across the adhesive-patch interface. Furthermore these shear stresses τ_{xz}, and τ_{yz} are zero at a free surface or at a plane of symmetry, and it is reasonable to assume that, since the patch and the sheet are thin, these stresses vary linearly with thickness in the patch and the sheet. With these assumptions the distribution of the shear stresses τ_{xz} and τ_{yz} is found to be:

$$\tau_{xz},\ \tau_{yz} = \frac{2z}{t_s}\,\tau_{sx},\ \tau_{sy} \text{ for } z \leqslant \frac{t_s}{2}$$

$$= \tau_{sx},\ \tau_{sy} \text{ for } \frac{t_s}{2} \leqslant z \leqslant \frac{t_s}{2}+t_a$$

$$= \frac{1}{t_o}\left(\frac{t_s}{2}+t_a+t_o-z\right)\tau_{sx},\ \tau_{sy}, \text{ for } \frac{t_s}{2}+t_a \leqslant z \leqslant \frac{t_s}{2}+t_a+t_o$$

where τ_{sx}, τ_{sy} are the shear stresses in the adhesive and are assumed constant through the thickness of the adhesive. The $z = 0$ plane is taken at the mid-surface of the sheet for a doubly reinforced sheet and at the lower surface of the sheet for a singly reinforced sheet. Here t_o, t_a are the thicknesses of the patch and adhesive respectively while t_s is the thickness of the sheet in the doubly reinforced case and is twice the sheet thickness in the singly reinforced case. This stress distribution is shown in Figure 1.

In what follows, we will confine our attention to the symmetrically patched sheet but we note that the results can also be applied, with only minor modifications, to a singly reinforced sheet of thickness $t_s/2$.

---

1. R. Jones and R. J. Callinan — On the use of special crack tip elements in cracked elastic sheets, Int. J. Fract., vol. 13, no. 1, pp. 51–64, 1977.
2. R. Jones and R. J. Callinan — A finite element method for calculating stress intensity factors in cracked sheets, A.R.L. Structures Report 360, Jan. 1977.

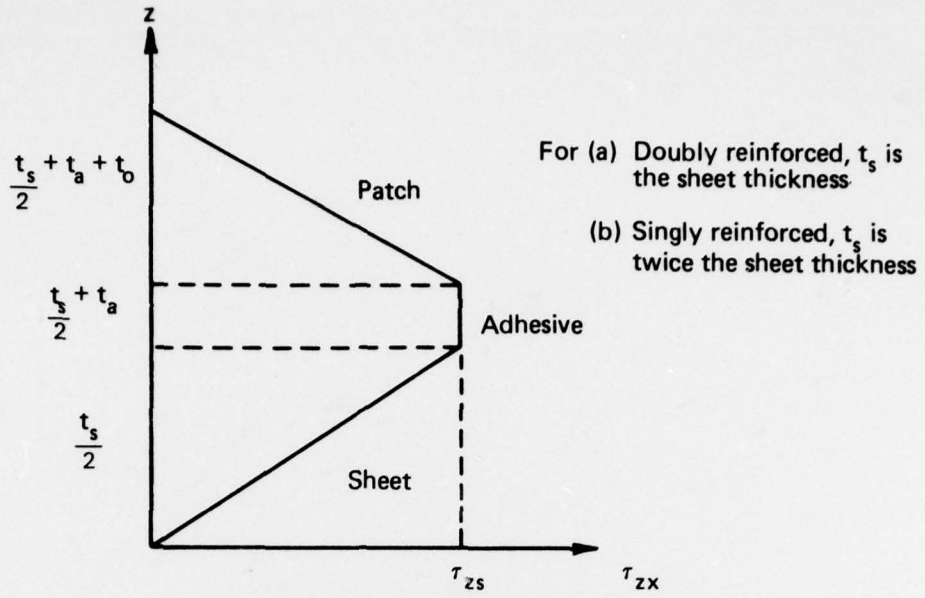

FIG. 1 DISTRIBUTION OF SHEAR STRESS THROUGH THICKNESS OF PATCHED SHEET

Let us now consider the x–y axes to be at some angle θ to the axes of orthotropy, denoted by $x'y'$, for the composite patch (see figure 2).

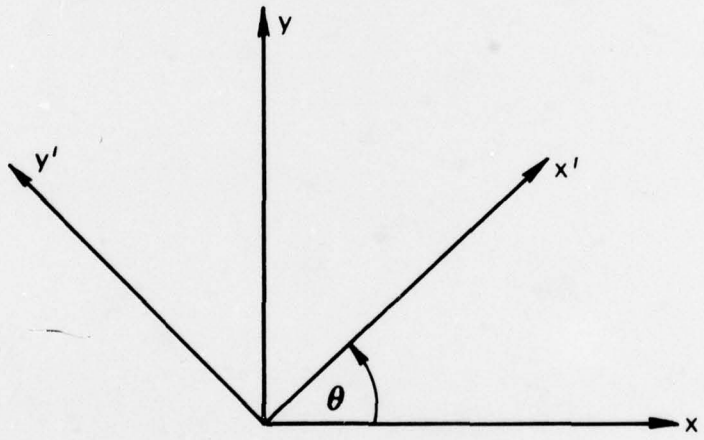

FIG. 2 AXIS SYSTEM IN PATCH

In the patch material the transverse shear stresses $\tau_{x'z}$, $\tau_{y'z}$ are related to the shear strains $\gamma_{x'z}$, $\gamma_{y'z}$ through the formulae

$$\tau_{x'z} = G'_{13}\,\gamma_{x'z} \tag{2.1}$$

$$\tau_{y'z} = G'_{23}\,\gamma_{y'z} \tag{2.2}$$

where G'_{13} and G'_{23} are the interlaminar shear moduli for the patch, while the shear stresses τ_{xz}, τ_{yz} are related to $\tau_{x'z}$, $\tau_{y'z}$ as follows:

$$\tau_{xz} = \tau_{x'z}\cos\theta - \tau_{y'z}\sin\theta \tag{2.3}$$

$$\tau_{yz} = \tau_{x'z}\sin\theta + \tau_{y'z}\cos\theta \tag{2.4}$$

Hence substituting equations (2.1) and (2.2) into (2.3) and (2.4) we obtain

$$\tau_{xz} = G'_{13}\,\gamma_{x'z}\cos\theta - G'_{23}\,\gamma_{y'z}\sin\theta \tag{2.5}$$

$$\tau_{yz} = G'_{13}\,\gamma_{x'z}\sin\theta + G'_{23}\,\gamma_{y'z}\cos\theta \tag{2.6}$$

However,

$$\gamma_{x'z} = \gamma_{xz}\cos\theta + \gamma_{yz}\sin\theta \tag{2.7}$$

$$\gamma_{y'z} = -\gamma_{xz}\sin\theta + \gamma_{yz}\cos\theta \tag{2.8}$$

so that on substituting for $\gamma_{x'z}$ and $\gamma_{y'z}$ into (2.5) and (2.6) we finally obtain

$$\tau_{xz} = G'_{13}\,(\gamma_{xz}\cos^2\theta + \gamma_{yz}\sin\theta\cos\theta) - G'_{23}\,(\gamma_{yz}\cos\theta\sin\theta - \gamma_{xz}\sin^2\theta) \tag{2.9}$$

$$\tau_{yz} = G'_{13}\,(\gamma_{xz}\cos\theta\sin\theta + \gamma_{yz}\sin^2\theta) + G'_{23}\,(\gamma_{yz}\cos^2\theta - \gamma_{xz}\sin\theta\cos\theta) \tag{2.10}$$

Now,

$$\gamma_{xz} = \frac{\partial u}{\partial z}, \quad \gamma_{yz} = \frac{\partial v}{\partial z} \tag{2.11}$$

where u and v are the horizontal components of displacement in the x and y directions respectively.

Substituting for τ_{xz}, and τ_{yz}, as given by equation (2.1), and for γ_{xz} and γ_{yz}, as given by equation (2.11), yields

$$f(z)\,\tau_{sy} = \frac{\partial u}{\partial z} f_1(\theta) + \frac{\partial v}{\partial z} f_2(\theta) \tag{2.12}$$

$$f(z)\,\tau_{sx} = \frac{\partial u}{\partial z} f_3(\theta) + \frac{\partial v}{\partial z} f_1(\theta) \tag{2.13}$$

where

$$\left.\begin{aligned} f_1(\theta) &= (G'_{13} - G'_{23})\sin\theta\cos\theta \\ f_2(\theta) &= G'_{23}\cos^2\theta + G'_{13}\sin^2\theta \\ f_3(\theta) &= (G'_{13}\cos^2\theta + G'_{23}\sin^2\theta) \\ f(z) &= \frac{1}{t_o}\left(\frac{t_s}{2} + t_a + t_o - z\right) \end{aligned}\right\} \tag{2.14}$$

and where, since we are examining the patch behaviour $t_a + t_s/2 \leqslant z \leqslant t_a + t_o + t_s/2$. If we multiply equation (2.12) by $f_1(\theta)$ and equation (2.13) by $f_2(\theta)$ and subtract we obtain

$$[f_1^2(\theta) - f_2(\theta)\,f_3(\theta)]\frac{\partial u}{\partial z} = f(z)\,[f_1(\theta)\,\tau_{sy} - f_2(\theta)\,\tau_{sx}] \tag{2.15}$$

Similarly upon multiplying equation (2.12) by $f_3(\theta)$ and (2.13) by $f_1(\theta)$ and subtracting we obtain

$$[f_1^2 - f_2 f_3]\frac{\partial v}{\partial z} = f(z)\,[f_1\tau_{sx} - f_3\tau_{sy}] \tag{2.16}$$

Recalling that $f(z) = (t_s/2 + t_a + t_o - z)/t_o$ and integrating equation (2.15) with respect to z yields

$$u(x, y, z) = \frac{z}{t_o}\left(\frac{t_s}{2} + t_a + t_o - \frac{z}{2}\right)\frac{(f_1\tau_{sy} - f_2\tau_{sx})}{(f_1^2 - f_2 f_3)} + h(x, y) \tag{2.17}$$

where $h(x, y)$ is an arbitrary function of x and y. If we now denote the movements of the mid-surface of the patch by u_o, v_o, i.e.,

$$\left.\begin{aligned} u_o &= u(x, y, z) \quad \text{at} \quad z = \frac{t_s}{2} + t_a + \frac{t_o}{2} \\ v_o &= v(x, y, z) \quad \text{at} \quad z = \frac{t_s}{2} + t_a + \frac{t_o}{2} \end{aligned}\right\} \tag{2.18}$$

we then see that

$$u_o = \left(\frac{t_s}{2} + t_a + \frac{t_o}{2}\right)\left(\frac{t_s}{4} + \frac{t_a}{2} + \frac{3t_o}{4}\right)\frac{(f_1\tau_{sy} - f_2\tau_{sx})}{(f_1^2 - f_2f_3)t_o} + h(x, y) \tag{2.19}$$

so that

$$h(x, y) = u_o - \left(\frac{t_s}{2} + t_a + \frac{t_o}{2}\right)\left(\frac{t_s}{4} + \frac{t_a}{2} + \frac{3t_o}{4}\right)\frac{(f_1\tau_{sy} - f_2\tau_{sx})}{(f_1^2 - f_2f_3)t_o} \tag{2.20}$$

and hence

$$u = u_o + \frac{(f_1\tau_{sy} - f_2\tau_{sx})}{(f_1^2 - f_2f_3)t_o}\left\{z\left(\frac{ts}{2} + t_a + t_o - \frac{z}{2}\right) - \left(\frac{ts}{2} + t_a + \frac{t_o}{2}\right)\left(\frac{t_s}{4} + \frac{t_a}{2} + \frac{3t_o}{4}\right)\right\} \tag{2.21}$$

Similarly we find that

$$v = v_o + \frac{[f_1\tau_{sx} - f_3\tau_{sy}]}{(f_1^2 - f_2f_3)t_o}\left\{z\left(\frac{t_s}{2} + t_a + t_o - \frac{z}{2}\right) - \left(\frac{t_s}{2} + t_a + \frac{t_o}{2}\right)\left(\frac{t_s}{4} + \frac{t_a}{2} + \frac{3t_o}{4}\right)\right\} \tag{2.22}$$

The u and v displacements at the patch-adhesive interface $z = t_s/2 + t_a$ are therefore found to be

$$u = u_o + \frac{(f_1\tau_{sy} - f_2\tau_{sx})}{(f_1^2 - f_2f_3)t_o}\left\{\left(\frac{t_s}{2} + t_a\right)\left(\frac{t_s}{4} + \frac{t_a}{2} + t_o\right) - \left(\frac{t_s}{2} + t_a + \frac{t_o}{2}\right)\left(\frac{t_s}{4} + \frac{t_a}{2} + \frac{3t_o}{4}\right)\right\} \tag{2.23}$$

and

$$v = v_o + \frac{(f_1\tau_{sx} - f_3\tau_{sy})}{(f_1^2 - f_2f_3)t_o}\left\{\left(\frac{t_s}{2} + t_a\right)\left(\frac{t_s}{4} + \frac{t_a}{2} + t_o\right) - \left(\frac{t_s}{2} + t_a + \frac{t_o}{2}\right)\left(\frac{t_s}{4} + \frac{t_a}{2} + \frac{3t_o}{4}\right)\right\} \tag{2.24}$$

Let us now turn our attention to the shear stress, and the displacements, in the sheet which we consider to be isotropic. In this case

$$\left.\begin{aligned}\frac{\partial u}{\partial z} &= \frac{1}{G_s}\tau_{xz}\\ \frac{\partial v}{\partial z} &= \frac{1}{G_s}\tau_{yz}\end{aligned}\right\} \tag{2.25}$$

where G_s is the shear modulus of the sheet. Substituting for the shear stresses τ_{xz}, τ_{yz} as given by equations (2.1) and integrating with respect to z we obtain

$$u = \frac{z^2}{G_s t_s}\tau_{sx} + g(x, y) \tag{2.26}$$

where $g(x, y)$ is an arbitrary function of x, y. Denoting the displacements of the mid-surface of the sheet (i.e. $z = 0$) by u_s, v_s we obtain

$$u_s = g(x, y) \tag{2.27}$$

so that

$$u = u_s + \frac{z^2\tau_{sx}}{G_s t_s} \tag{2.28}$$

and similarly

$$v = v_s + \frac{z^2\tau_{sy}}{G_s t_s} \tag{2.29}$$

The maximum value of the displacements occur at the sheet adhesive interface, $z = t_s/2$, and have the values

$$u = u_s + \frac{t_s\,\tau_{sx}}{4G_s} \tag{2.30}$$

$$v = v_s + \frac{t_s \tau_{sy}}{4G_s} \tag{2.31}$$

We now know the displacements at the interfaces of the patch-adhesive and sheet-adhesive, and are in a position to evaluate the shear strain and shear stress in the adhesive. Let us begin by assuming an isotropic adhesive in which, as mentioned earlier, the shear stresses τ_{xz} and τ_{yz} take a constant value across the thickness of the adhesive. Since the adhesive is isotropic we know that

$$\frac{\tau_{sx}}{G_a} = \frac{\partial u}{\partial z} = \frac{u(x, y, t_s/2 + t_a) - u(x, y, t_s/2)}{t_a} \tag{2.32}$$

and

$$\frac{\tau_{sy}}{G_a} = \frac{\partial v}{\partial z} = \frac{v(x, y, t_s/2 + t_a) - v(x, y, t_s/2)}{t_a} \tag{2.33}$$

where G_a is the shear modulus of the adhesive, and where $u(x, y, t_s/2)$, $v(x, y, t_s/2)$ are the values of the displacement at the sheet-adhesive interface as given by equations (2.30) and (2.31) while $u(x, y, t_s/2 + t_a)$, $v(x, y, t_s/2 + t_a)$ are the displacements at the adhesive-patch interface, as given by equations (2.23) and (2.24). Substituting these values into equations (2.32) and (2.33) and collecting terms we finally obtain

$$u_o - u_s = \tau_{sx}\left\{\left(\frac{t_a}{G_a} + \frac{t_s}{4G_s}\right) - \frac{3t_o f_2}{8(f_1^2 - f_2 f_3)}\right\} + \frac{3t_o f_1 \tau_{sy}}{8(f_1^2 - f_2 f_3)} \tag{2.34}$$

and

$$v_o - v_s = \tau_{sy}\left\{\left(\frac{t_a}{G_a} + \frac{t_s}{4G_s}\right) - \frac{3t_o f_3}{8(f_1^2 - f_2 f_3)}\right\} + \frac{3t_o f_1 \tau_{sx}}{8(f_1^2 - f_2 f_3)} \tag{2.35}$$

These can be solved for τ_{sx} and τ_{sy}, giving

$$\tau_{sx} = \frac{f_6(u_o - u_s)}{(f_5 f_6 - f_4^2)} + \frac{f_4(v_o - v_s)}{(f_5 f_6 - f_4^2)} \tag{2.36}$$

$$\tau_{sy} = \frac{f_4(u_o - u_s)}{(f_5 f_0 - f_4^2)} + \frac{f_5(v_o - v_s)}{(f_5 f_6 - f_4^2)} \tag{2.37}$$

where for convenience we have denoted

$$\left.\begin{aligned} f_4 &= \frac{3t_o f_1}{8(f_2 f_3 - f_1^2)} \\ f_5 &= \frac{t_a}{G_a} + \frac{t_s}{4G_s} - \frac{3t_o f_2}{8(f_1^2 - f_2 f_3)} \\ f_6 &= \frac{t_a}{G_a} + \frac{t_s}{4G_s} - \frac{3t_o f_3}{8(f_1^2 - f_2 f_3)} \end{aligned}\right\} \tag{2.38}$$

(Note that for the case of a singly reinforced sheet the term $t_s/4G_s$ in the expressions for f_5 and f_6 have to be replaced by $3t_s/8G_s$).

We thus see that for a composite patch bonded to an elastic isotropic sheet the shear stress developed in the adhesive depends upon both of the relative displacements $(u_o - u_s)$ and $(v_o - v_s)$ between the patch and the sheet. In the case when $G'_{13} = G'_{23}$ $(= G_0)$, which only occurs when the patch is transversely isotropic, then the analysis simplifies considerably. In this case

$$\begin{aligned} f_1(\theta) &= 0 \\ f_2(\theta) &= G_0 \\ f_3(\theta) &= G_0 \\ f_4 &= 0 \end{aligned}$$

$$f_5 = f_6 = \frac{t_a}{G_a} + \frac{t_s}{4G_s} + \frac{3t_o}{8G_o} \tag{2.39}$$

so that

$$\tau_{sx} = \frac{(u_o - u_s)}{\left(\frac{t_a}{G_a} + \frac{t_s}{4G_s} + \frac{3t_o}{8G_o}\right)} \tag{2.40}$$

$$\tau_{sy} = \frac{(v_o - v_s)}{\left(\frac{t_a}{G_a} + \frac{t_s}{4G_s} + \frac{3t_o}{8G_o}\right)} \tag{2.41}$$

In this case the shear stress τ_{sx} depends only on the quantity $u_o - u_s$, while τ_{sy} depends only on $v_o - v_s$. Such a behaviour is known to occur when the patch is isotropic. However in analysing the effect of stiffeners on crack growth several investigators—e.g. Arin[3,4]—have assumed the relationship to have the form

$$\tau_{sx} = \frac{G_a}{t_a}(u_o - u_s) \tag{2.42}$$

$$\tau_{sy} = \frac{G_a}{t_a}(v_o - v_s) \tag{2.43}$$

In so doing they have effectively neglected the contributions of the terms $t_s/4G_s + 3t_o/8G_o$. An estimate of the error involved in their approximation may be obtained by considering a Boron-epoxy laminate of thickness 0·508 mm bonded to a 2·286 mm thick aluminium sheet the thickness of the adhesive being 0·1016 mm. The material parameters for the Boron-epoxy are $G_{13} = 7{\cdot}24 \times 10^3$ MPa while the shear modulus of the adhesive and the aluminium are $9{\cdot}65 \times 10^2$ MPa and $27{\cdot}3 \times 10^3$ MPa respectively. These values correspond to a fairly typical patch configuration. This gives the value of G_a/t_a as $9{\cdot}50 \times 10^3$ MPa/mm while the ratio $1\Big/\left(\frac{t_a}{G_a} + \frac{t_s}{4G_s} + \frac{3t_o}{8G_o}\right)$ takes on the value $6{\cdot}56 \times 10^3$ MPa/mm, where for the sake of comparison we have approximated G_{23} by G_{13} thus assuming the patch to be transversely isotropic. The error introduced by using the simple formulae (2.42) and (2.43) for the shear stresses is therefore 45%. This casts doubts on the results and conclusions of those investigations, such as those of Arin[3,4], which utilize these simple formulae. Indeed any analysis based upon equations (2.42) and (2.43) will significantly overestimate the load transmitted to the patch and consequently underestimate the stress intensity factor.

It is interesting to note that a relationship similar to that given by equations (2.40) and (2.41) is also presented by Mitchell et al.[5] although no exact derivation is given there.

It is important to note that, unlike references [3, 4, 5], the present analysis clearly shows that the shear stress in the adhesive τ_{sx} (and similarly τ_{sy}) is influenced by the relative motions of the sheet and the patch in both the x and y directions.

Let us now turn our attention to the case of a patch which has $G_{13} \approx G_{23}$ $(= G_0)$ and for which the shear stresses in the adhesive are given by equations (2.40) and (2.41). We may now substitute these expressions for the shear stresses into equations (2.30) and (2.31) and obtain the following expressions for displacements in the sheet, viz.

---

3. K. Arin — A plate with a crack stiffened by a partially debonded Stringer. Eng. Frac. Mech., vol. 6, pp. 133–140, 1974.

4. K. Arin — A note on the effect of lateral bending stiffness of stringers attached to a plate with a crack. Eng. Fract. Mech. vol. 7, no. 1, pp. 173–179, 1975.

5. R. A. Mitchell, R. M. Wooley and D. J. Chivirut — Analysis of composite-reinforced cutouts and cracks. A.I.A.A., 13, 6, 744–749 (1975).

$$u(x, y, z) = u_s + z^2 K_s(u_o - u_s)/t_s G_s \tag{2.44}$$

$$v(x, y, z) = v_s + z^2 K_s(v_o - v_s)/t_s G_s \tag{2.45}$$

where for convenience we have written

$$K_s = 1\Big/\left(\frac{t_a}{G_a} + \frac{t_s}{4G_s} + \frac{3t_o}{8G_o}\right) \tag{2.46}$$

The mean stress in the sheet is thus given by

$$\begin{aligned}\sigma_x &= \frac{E_s}{(1-\nu_s^2)t_s}\int_{-t_s/2}^{t_s/2}(\epsilon_x + \nu_s\epsilon_y)dz \\ &= \left(1 - \frac{K_s t_s}{12G_s}\right)\frac{E_s}{(1-\nu_s^2)}\left(\frac{\partial u_s}{\partial x} + \frac{\nu\partial v_s}{\partial y}\right) + \frac{K_s t_s E_s}{12G_s(1-\nu_s^2)}\left(\frac{\partial u_o}{\partial x} + \frac{\nu\partial v_o}{\partial y}\right) \\ &= \left(1 - \frac{K_s t_s}{12G_s}\right)\sigma_{sx} + \frac{K_s t_s E_s(\epsilon_{ox} + \nu_s\epsilon_{oy})}{12G_s(1-\nu_s^2)}\end{aligned} \tag{2.47}$$

and similarly

$$\sigma_y = \frac{E_s}{(1-\nu_s^2)t_s}\int_{-t_s/2}^{t_s/2}(\epsilon_y + \nu_s\epsilon_x)dz = \left(1 - \frac{K_s t_s}{12G_s}\right)\sigma_{sy} + \frac{K_s t_s E_s(\epsilon_{oy} + \nu_s\epsilon_{ox})}{12G_s(1-\nu_s^2)} \tag{2.48}$$

$$\tau_{xy} = \frac{G_s}{t_s}\int_{-t_s/2}^{t_s/2}\gamma_{xy}dz = \left(\frac{1 - K_s t_s}{12G_s}\right)\tau_{sxy} + \frac{K_s t_s}{12}\gamma_{oxy} \tag{2.49}$$

where ν_s and E_s are the Poisson's ratio and the Young's modulus for the sheet, τ_{sxy}, σ_{sx}, σ_{sy} are the stresses in the sheet as predicted by the theory of plane stress (i.e. when the transverse shear stresses are neglected) and γ_{oxy}, ϵ_{ox}, ϵ_{oy} are the strains in the patch.

In the case of a cracked sheet the strains in the patch are finite while the stresses at the crack tip are infinite so that at the crack tip

$$\begin{aligned}\sigma_x &= \left(1 - \frac{K_s t_s}{12G_s}\right)\sigma_{sx} \\ \sigma_y &= \left(1 - \frac{K_s t_s}{12G_s}\right)\sigma_{sy} \\ \tau_{xy} &= \left(1 - \frac{K_s t_s}{12G_s}\right)\tau_{sxy}\end{aligned}$$

Hence for a patched crack the result of including effects of the transverse shear stress in the sheet itself is to reduce the stress intensity factors by the factor $(1 - (t_s K_s/12G_s))$. For most practical situations this reduction will only be of the order of a few per cent. Nevertheless this is an important result as it shows that the usual procedure of neglecting the shear stresses τ_{zx} and τ_{zy} in the sheet is conservative as regards estimates of the stress intensity factors and hence slightly underestimates the load required for crack initiation. For example for the patch discussed earlier $K_s = 6{\cdot}56 \times 10^3$ MPa/mm, $t_s = 2{\cdot}286$ mm, $G_s = 27{\cdot}3 \times 10^3$ MPa and $1 - (t_s K_s/12G_s) = 0{\cdot}954$, the reduction in the stress intensity factor thus being only 4·6 per cent. Consequently when producing a numerical model for the crack patching problem we can neglect the effects of the transverse shear stresses in the sheet and in the patch with little loss in accuracy.

The finite element technique for analysing the crack-patching problem will be developed in the next section.

3. A FINITE ELEMENT APPROACH TO CRACK PATCHING

In the previous Section we have seen that transverse shear stresses τ_{xz} and τ_{yz} in the patch and the sheet may be neglected; hence the stiffness matrices for elements in the sheet and in the patch may be computed using standard finite element routines for membrane-type elements. It is

the stiffness matrix of the adhesive which couples these two stiffness matrices together. We will therefore turn our attention to determining the stiffness matrix for an element of adhesive.

The strain energy V_a of an element of the adhesive is given by

$$V_a = \frac{1}{2G_a}\int_{t_s/2}^{t_s/2+t_a}\iint_e (\tau_{zx}^2 + \tau_{zy}^2)dxdydz = \frac{t_a}{2G_a}\iint_e (\tau_{zx}^2 + \tau_{zy}^2)dxdy \qquad (3.1)$$

where the double integration is over the area of the element. The element stiffness matrix, K_a^e for the adhesive is now obtained by first prescribing the form of the shear stress variation within the element and then by differentiating the strain energy with respect to each of the elemental degrees of freedom. However before prescribing the nature of the shear stresses we must first stipulate the geometry of the element to be considered. Here we will confine our attention to triangular elements which are the basic elements from which all other elements may be assembled. Let us assume that, within the element, the shear stresses vary linearly with x and y, i.e.,

$$\tau_{zx} = [(a_i + b_i x + c_i y)\tau_{zxi} + (a_j + b_j x + c_j y)\tau_{zxj} + (a_m + b_m x + c_m y)\tau_{zxm}]/2\Delta \qquad (3.2)$$

where

$$\left.\begin{aligned} a_i &= x_j y_m - x_m y_j \\ b_i &= y_j - y_m \\ c_i &= x_m - x_j \end{aligned}\right\} \qquad (3.3)$$

and a_j, a_m, b_j, b_m and c_j, c_m are obtained by a cyclic permutation of the indices i, j, m. Here (x_i, y_i), (x_j, y_j) and (x_m, y_m) are the coordinates of the corners of the element, Δ is the area of the element and τ_{zxi}, τ_{zxj}, τ_{zxm} are the values of the shear stresses at the nodes i, j and m respectively (see Figure 3). Hence if we now substitute for τ_{zxi}, τ_{zxj} and τ_{zxm} as given by equations (2.36) we obtain

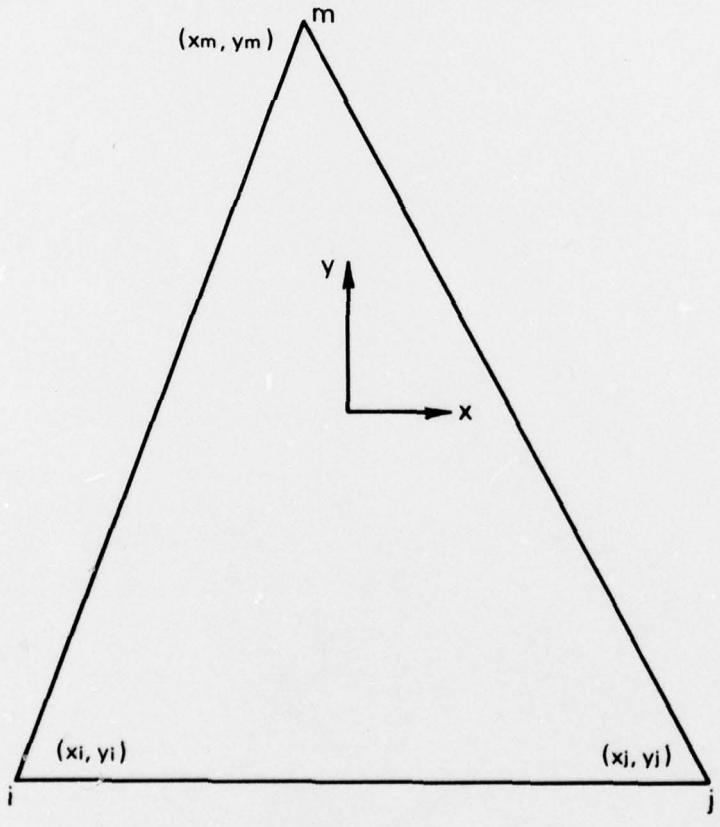

FIG. 3 ELEMENT OF ADHESIVE

$$\tau_{zx} = \frac{(a_i + b_i x + c_i y)}{2\Delta(f_5 f_6 - f_4^2)}[f_6(u_o - u_s)_i + f_4(v_o - v_s)_i]$$
$$+ \frac{(a_j + b_j x + c_j y)}{(f_5 f_6 - f_4^2)2\Delta}[f_6(u_o - u_s)_j + f_4(v_o - v_s)_j]$$
$$+ \frac{(a_m + b_m x + c_m y)}{2\Delta(f_5 f_6 - f_4^2)}[f_6(u_o - u_s)_m + f_4(v_o - v_s)_m]$$
$$= \frac{1}{(f_5 f_6 - f_4^2)} \sum_{p=i,j,m} \phi_p(x, y)[f_6(u_o - u_s)_p + f_4(v_o - v_s)_p] \qquad (3.4)$$

similarly,

$$\tau_{zy} = \frac{(a_i + b_i x + c_i y)}{(f_5 f_6 - f_4^2)2\Delta}[f_4(u_o - u_s)_i + f_5(v_o - v_s)_i]$$
$$+ \frac{(a_j + b_j x + c_j y)}{(f_5 f_6 - f_4^2)2\Delta}[f_4(u_o - u_s)_j + f_5(v_o - v_s)_j]$$
$$+ \frac{(a_m + b_m x + c_m y)}{(f_5 f_6 - f_4^2)2\Delta}[f_4(u_o - u_s)_m + f_5(v_o - v_s)_m]$$
$$= \frac{1}{(f_5 f_6 - f_4^2)} \sum_{p=i,j,m} \phi_p(x, y)[f_4(u_o - u_s)_p + f_5(v_o - v_s)_p] \qquad (3.5)$$

where $\phi_i(x, y) = (a_i + b_i x + c_i y)/2\Delta$ and where p takes on the values i, j or m. Substituting for τ_{xz}, and τ_{yz} into equation (3.1) we obtain the following expression for the strain energy:

$$V_a = \frac{t_a}{2G_a} \iint [\mathrm{F}_1 \{\Sigma_p \phi_p(x, y)(u_o - u_s)_p\}^2 + \mathrm{F}_3 \{\Sigma_p \phi_p(x, y)(v_o - v_s)_p\}^2$$
$$+ 2\mathrm{F}_2 \{\Sigma_p \phi_p(x, y)(v_o - v_s)_p\}\{\Sigma_q \phi_q(x, y)(u_o - u_s)_q\}] \, dxdy \qquad (3.6)$$

Here p and q are dummy indices which take on the node values of either i, j or m and where, for the sake of convenience, we have written

$$\left.\begin{aligned} F_1 &= (f_4^2 + f_6^2)/(f_5 f_6 - f_4^2)^2 \\ F_2 &= f_4(f_5 + f_6)/(f_5 f_6 - f_4^2)^2 \\ F_3 &= (f_4^2 + f_5^2)/(f_5 f_6 - f_4^2)^2 \end{aligned}\right\} \qquad (3.7)$$

Equation (3.6) directly relates the strain energy of the adhesive to the displacements in the sheet and the patch and clearly illustrates the importance of the previous Section where the exact nature of the shear stress in the adhesive was determined.

The element stiffness matrix is now obtained by differentiating V_a with respect to each of the elemental degrees of freedom, i.e.

$$K^e{}_a \underset{\sim}{\lambda} = \frac{\partial V_a}{\partial \underset{\sim}{\lambda}} \qquad (3.8)$$

where $\underset{\sim}{\lambda}$ is the vector

$$\underset{\sim}{\lambda}^T = [u_{si}, v_{si}, u_{oi}, v_{oi}, u_{sj}, v_{sj}, u_{oj}, v_{oj}, u_{sm}, v_{sm}, u_{om}, v_{om}] \qquad (3.9)$$

This technique is explained in detail in references [1, 2], and the full form of the 12 × 12 stiffness matrix is given in Appendix I.

Having thus obtained the stiffness matrix for the adhesive, we now couple the stiffness matrix of the adhesive to the stiffness matrix of the composite patch and thus produce a stiffness matrix for the bonded patch-adhesive pair. This coupling is a very simple procedure since by specifying the degrees of freedom of the adhesive, i.e. $\underset{\sim}{\lambda}$, we immediately specify the position, in the matrix, of the terms due to the composite. For example in equation (3.9) we see that the u and v displacements in the patch occupy positions 3,4,7,8,11,12. Hence the first row in the stiffness matrix of the patch is located in the third row of the stiffness matrix for the bonded element, the first term

in the row occurring in position (3,3) the second term in position (3,4) the third term in (3,7) the fourth term in (3,8) the fifth in (3,11) and the last term in (3,12). The second row is relocated in the fourth row, the third row is relocated in the seventh row etc. An algorithm for doing this is given in Appendix II.

This bonded pair is now used in conjunction with standard finite element routines except at the crack tip where it is coupled to the special crack tip element developed by the author's in references [1, 2].

So far we have assumed a complete bond between the adhesive and the sheet. However sometimes one is faced with the situation where debonding of the patch from the sheet has occurred over some area. The present analysis can cover this case by allowing all or any of the nodal displacements at the lower interface of the adhesive to differ from the displacement in the sheet. In the case of a small debond on either side of the crack this requires correspondingly small elements, and hence a more complex mesh. To overcome this requirement for a fine mesh it is possible to modify the bonded element developed above with a nodal displacement vector $\underset{\sim}{\lambda}$, by forcing the displacement of the adhesive at the crack, to take the mean value of the displacement of the sheet at either side of the crack. In this case the nodal displacement vector is

$$\underset{\sim}{\lambda}^{\mathrm{T}} = [u_{si+}, v_{si+}, u_{oi}, v_{oi}, u_{sj}, v_{sj}, u_{oj}, v_{oj}, u_{sm}, v_{sm}, u_{om}, v_{om}, u_{si-}, v_{si-}] \tag{3.10}$$

where the ith node is assumed to be at the crack and where u_{si+}, and u_{si-} etc. are the values of the displacements on either side of the crack. The stiffness matrix $\bar{K}_a$ for this case is computed using the algorithm

$$\left.\begin{aligned} \bar{K}_a(m, n) &= K_a(m, n) \text{ for } m, n = 1 \text{ to } 12 \\ \bar{K}_a(m, n) &= \tfrac{1}{2}\bar{K}_a(m, n) \text{ for } m \leqslant 2, n \leqslant 12 \\ \bar{K}_a(m, n) &= \tfrac{1}{2}\bar{K}_a(m, n) \text{ for } m \leqslant 12, n \leqslant 2 \\ \bar{K}_a(m, 12 + n) &= \bar{K}_a(m, n) \text{ for } n \leqslant 2, m \leqslant 12 \\ \bar{K}_a(m + 12, n) &= \bar{K}_a(m, n) \text{ for } m \leqslant 2, n \leqslant 14 \end{aligned}\right\} \tag{3.11}$$

where $K_a(m, n)$ is the m, nth term of the stiffness matrix determined above assuming complete adhesion.

It is interesting to note that in the case of a centre cracked panel under uniform tension this results in the adhesive at the crack having zero displacement, whereas in the fully bonded situation the adhesive will move differently on either side of the crack. The latter results in a displacement discontinuity in the adhesive across the crack which, in turn, may result in the creation of a crack in the adhesive itself or may cause a localized debonding effect along the crack.

Having thus allowed for all possible effects we will now illustrate the use of the analytical tools developed above by considering a tension panel with a central crack which is reinforced by a Boron-epoxy patch and where we will concentrate on the reduction in the stress intensity factor caused by the patch; and on the stresses in the patch and the adhesive.

4. ILLUSTRATION OF THE METHOD

As mentioned in the last paragraph above, let us consider a thin rectangular sheet of dimensions 508 mm × 635 mm × 2·3 mm subjected to a uniform tensile stress of 689 KPa. The sheet contains a central crack 38·1 mm long which is patched on both sides and at both ends by a Boron-epoxy laminate placed directly over the crack tip. The laminate is uniaxial, the fibers lying perpendicular to the length of the crack, the lateral dimensions of the patch are 100·8 mm × 17·7 mm, and various thicknesses of patch are considered. The patch is bonded to the sheet with an adhesive of thickness 0·1016. The Young's modulus of the sheet is 71·02 × 10^3 MPa while the Poisson's ratio is 0·32. The moduli of the laminate are $G_{23} = 4{\cdot}94 \times 10^3$ MPa, $G_{13} = 7{\cdot}24 \times 10^3$ MPa, $E_1 = 208{\cdot}1 \times 10^3$ MPa, $E_1/E_2 = 8{\cdot}18$, $\nu_{12} = 0{\cdot}1677$ and the shear modulus of the adhesive is $G_a = 9{\cdot}65 \times 10^2$ MPa.

Because of the symmetrical nature of the problem only one half of the structure was analysed and the sheet was idealised as in figure 4 where in order to model accurately the stresses in the adhesive it was necessary to have a fairly fine mesh. Indeed, by modelling one half of the plate rather than only one quarter we are able to calculate both the mode I and mode II stress intensity

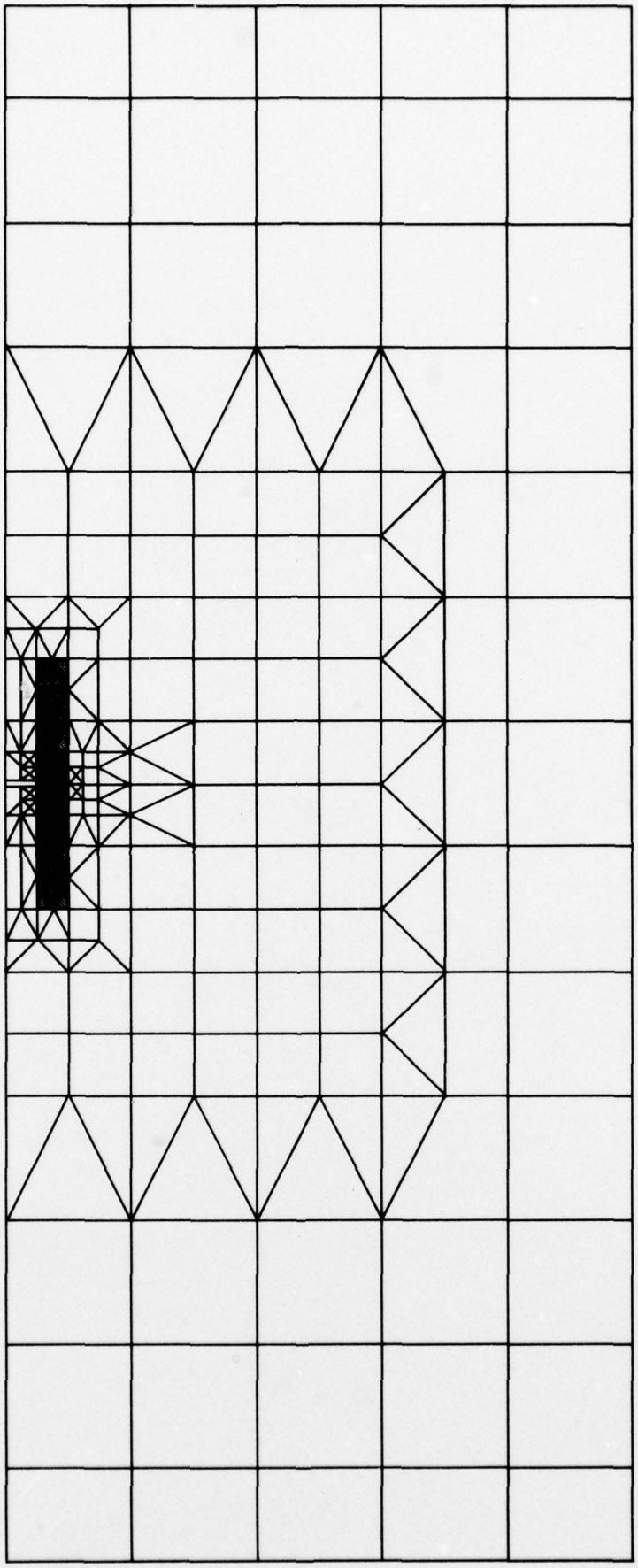

FIG. 4 FINITE ELEMENT GRID FOR HALF OF PATCHED PANEL

factors, K_1 and K_1, for the structure, as described in references [1,2] so that any error in the data can be detected by evaluating the ratio K_2/K_1. If the data are correct, then this ratio should be zero. However, because of the large amount of data and because of round-off effects, which accumulate during computation it was often found that the ratio was non zero. The maximum tolerated value of this ratio was 0·01, i.e. K_2 was not allowed to exceed 1% of K_1. Whenever K_2 did exceed this value it transpired there were data errors.

Table 1 shows the effect that increasing the patch thickness has upon the computed value of the stress intensity factor K_1, when no debond is present.

TABLE 1

Patch Thickness (mm)	K_1 (KPa.m$^{\frac{1}{2}}$)
0	166·2
0·127	77·8
0·254	65·0
0·381	57·9
0·508	53·1
0·762	46·7

It is interesting to note that, when the patch is not present, the method yields the value $K_1 = 166{\cdot}2$ kPa.m$^{\frac{1}{2}}$ which differs by only 1% from the exact analytical result[6] 168·5 kPa.m$^{\frac{1}{2}}$. From Table 1, we see that patching is a very efficient way of lowering the stress intensity factor, and that the addition of extra layers of the Boron-epoxy laminate continually decreases the value of the stress intensity factor. However, increasing the thickness of the laminate adversely effects the τ_{zy} shear stress in the adhesive as may be seen in Table 2 where the maximum shear stress developed in the adhesive at the ends of the patch, is shown for various patch thicknesses.

TABLE 2

Patch Thickness (mm)	τ_{zy} (kPa)
0·12	106
0·254	181
0·371	236
0·508	280
0·762	345

From this table it is apparent that increasing the thickness of the laminate from 0·5 mm to 0·76 mm (i.e. from four to six layers) results in an increase in the shear stress in the adhesive of 23% while only reducing K_1 by 12%.

Hence, when increasing the number of layers of the laminate one must be watchful of the detrimental effect it has in raising the shear stress in the adhesive. One must therefore be careful when using composite patches not to exceed the "optimum" number of layers.

Figures 5, 6, 7 and 8 show the complete variation of the shear stress throughout the adhesive for various thicknesses of the laminate. From these diagrams it is apparent that the shear stresses in the adhesive on the line of the crack at the right hand edge of the patch (i.e. outboard of the crack tip) are much smaller than those at the left hand edge of the patch (i.e. inboard of the crack tip). Also, the stresses at the right hand edge vary along the length of the patch in the same general fashion as in a lap joint.

---

6. G. C. Sih and H. Liebowitz — Mathematical Fundamentals, Fracture, Vol. 2, Academic Press, N.Y., 1969.

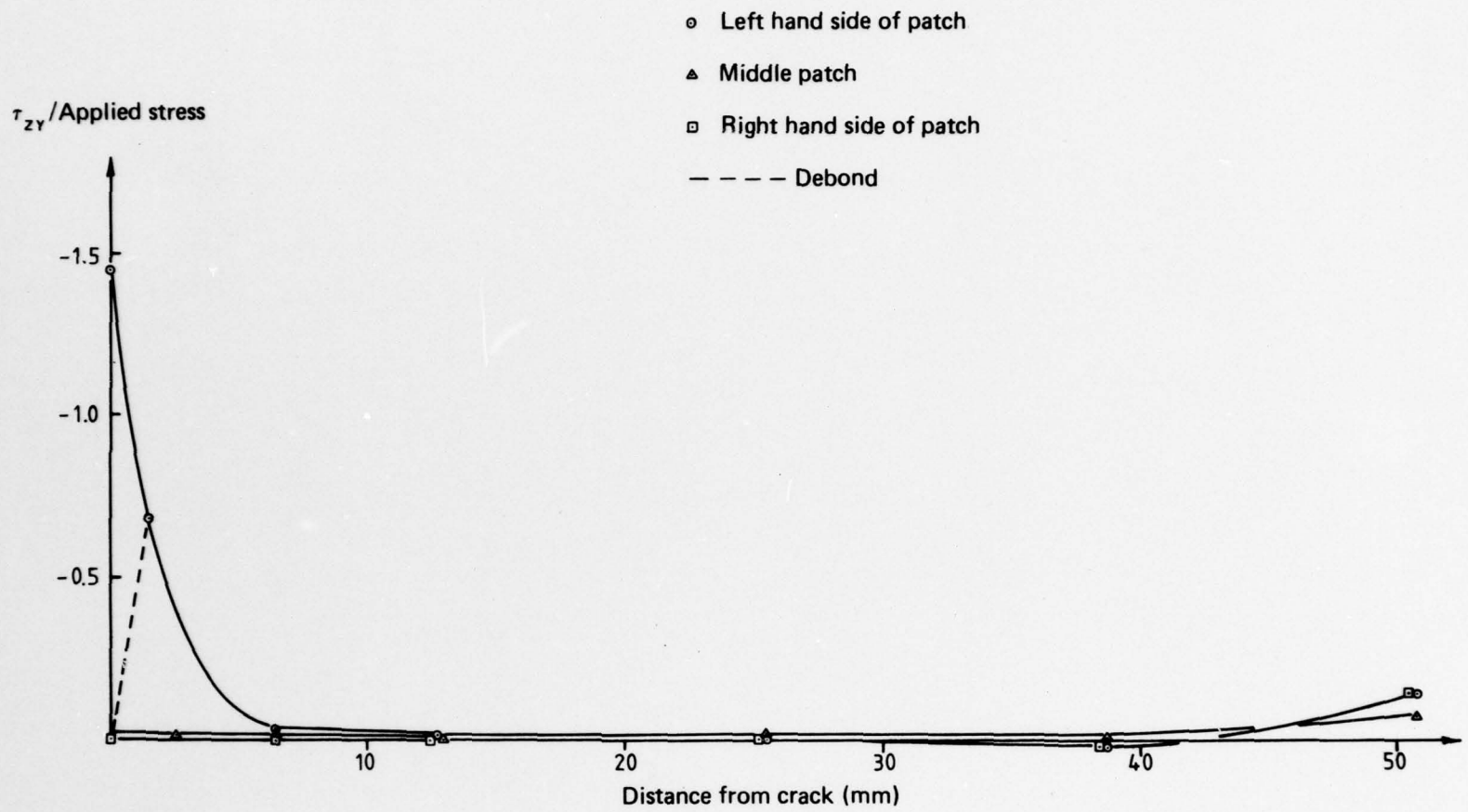

FIG. 5 VARIATION OF ADHESIVE SHEAR STRESS: THICKNESS OF PANEL = 0.012 / mm

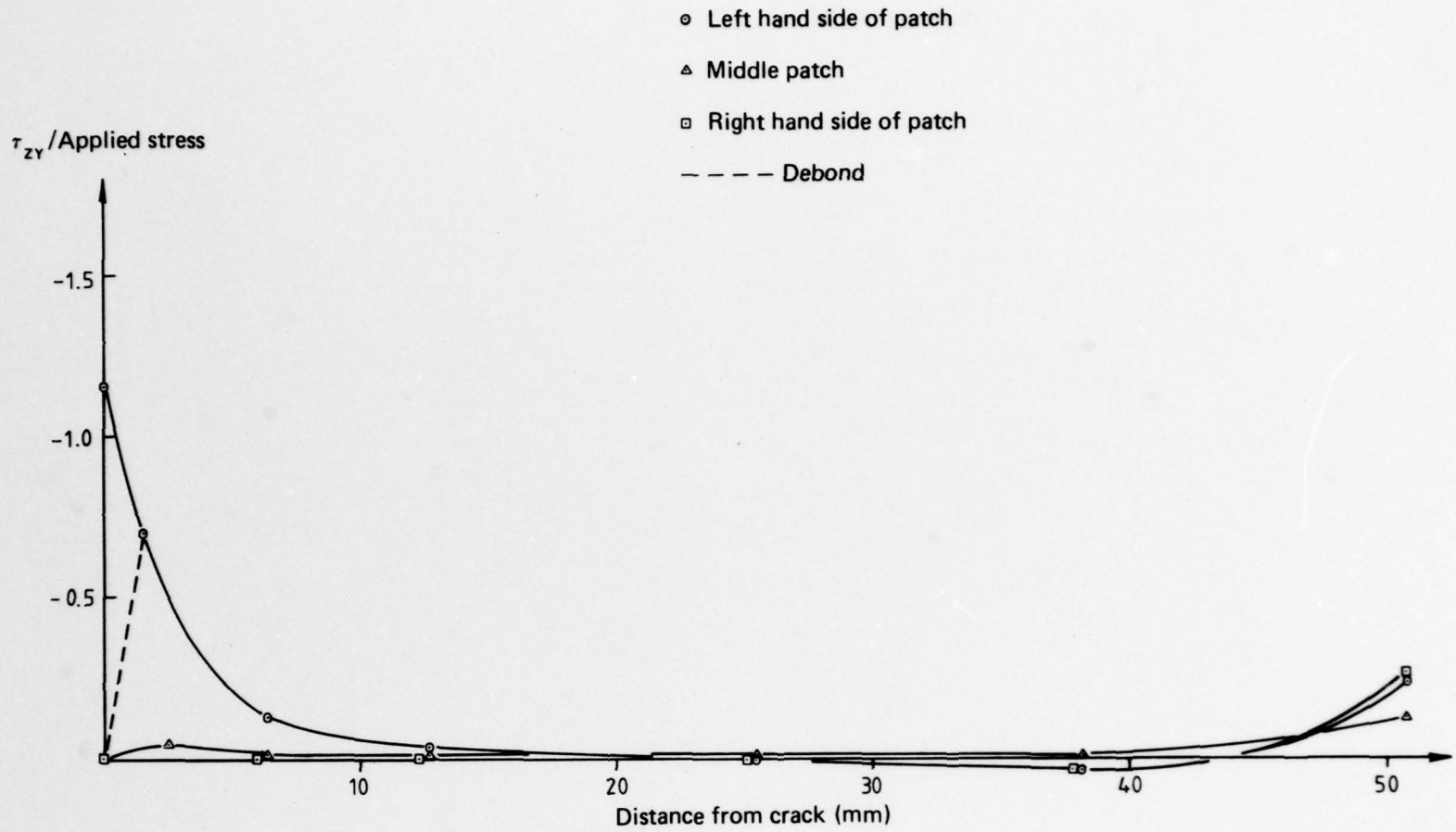

FIG. 6 VARIATION OF ADHESIVE SHEAR STRESS: THICKNESS OF PANEL = 0.2540 mm

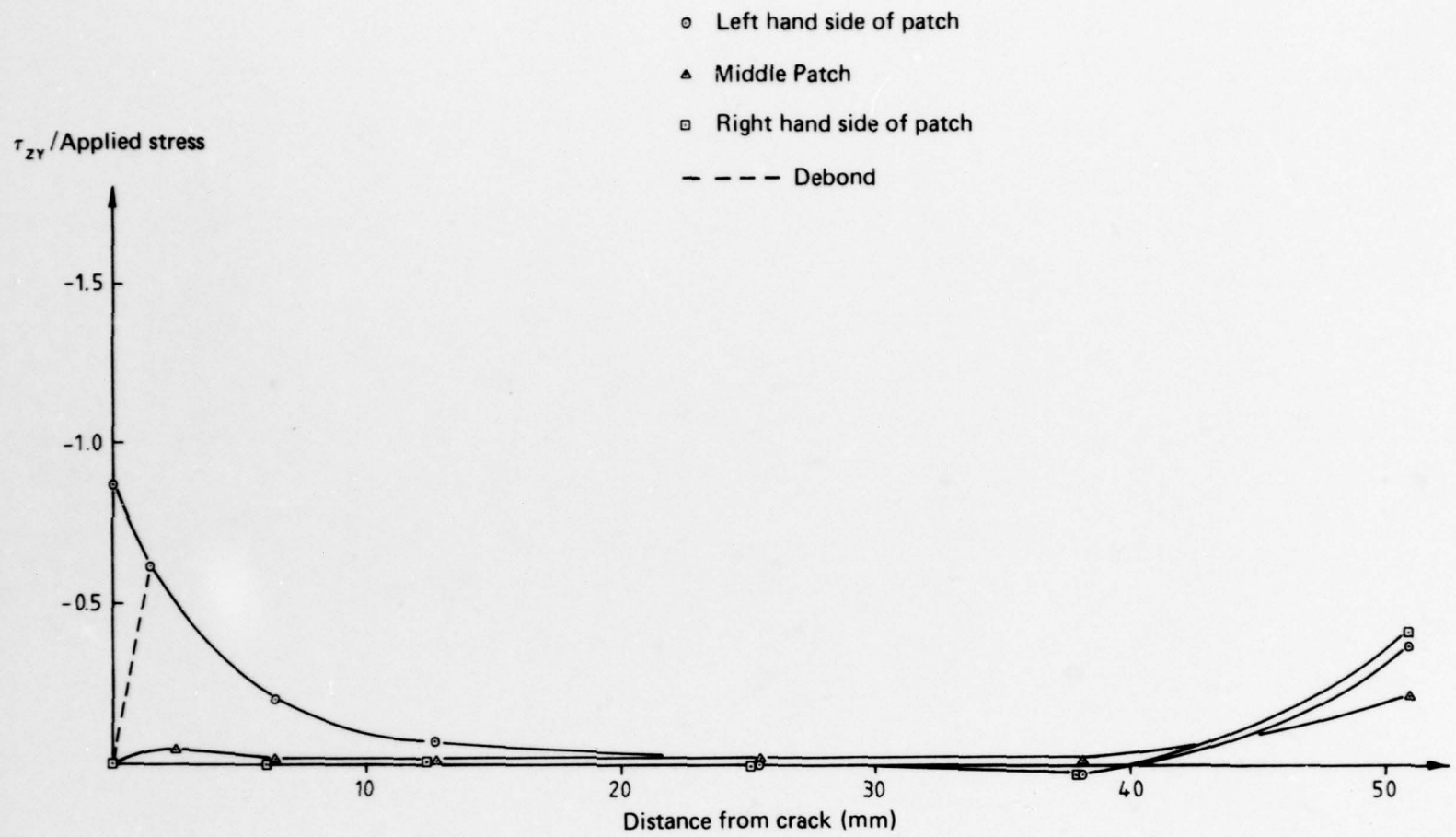

FIG. 7 VARIATION OF ADHESIVE SHEAR STRESS: THICKNESS OF PANEL = 0.5080 mm

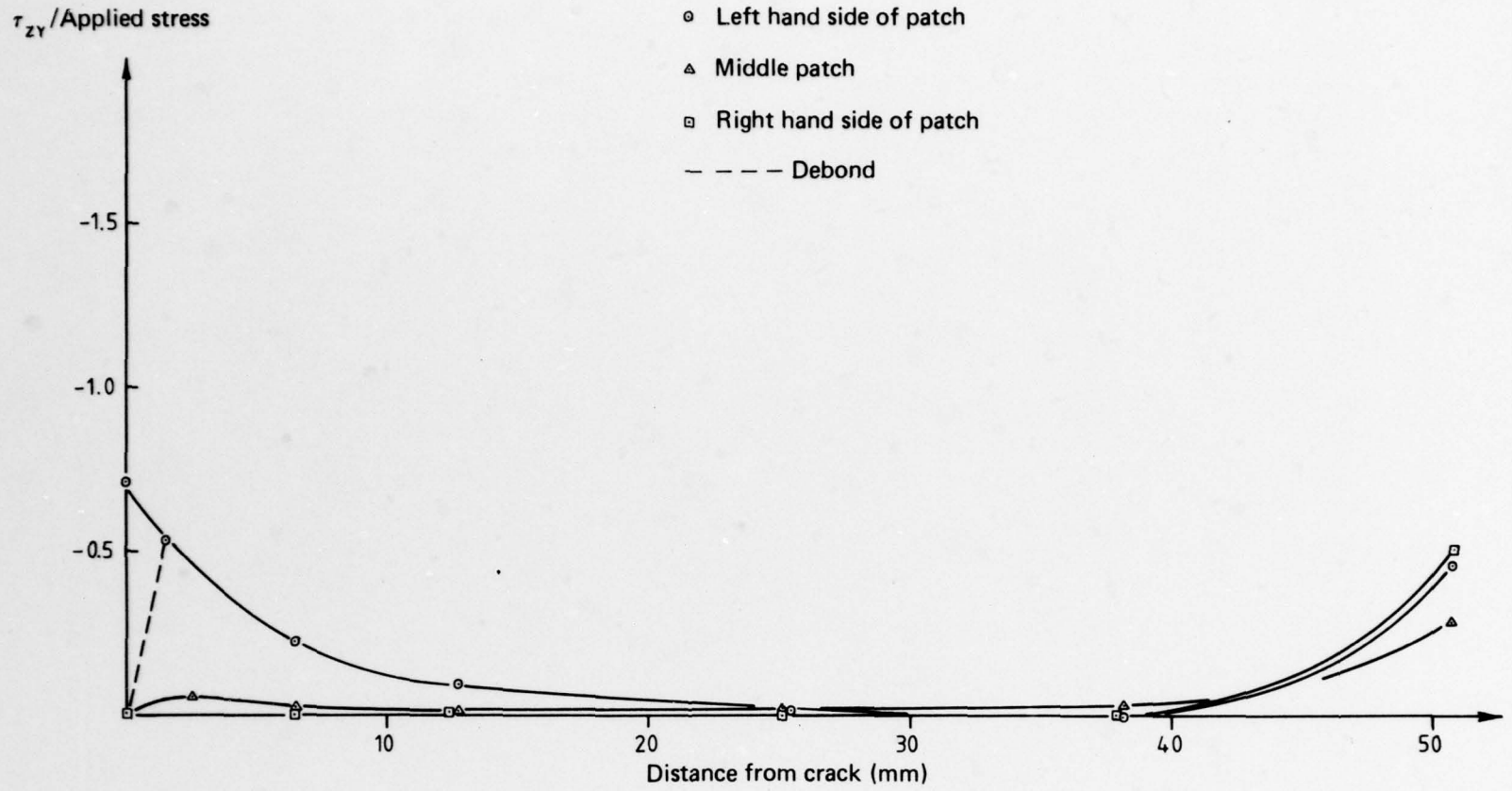

FIG. 8 VARIATION OF ADHESIVE SHEAR STRESS: THICKNESS OF PANEL = 0.762 mm

The stresses in the patch are predominantly σ_y stresses, i.e. $\sigma_x \approx \tau_{xy} \approx 0$, and are fairly constant across the width of the patch, the only exception being at the crack, i.e. on the x axis. These stresses are shown in Figure 9 where we see that for each thickness of patch the maximum stresses occur in the region of the crack and decay monotonically towards the edges of the patch. The maximum σ_y stress is shown in Table 3 for various thicknesses of the patch.

TABLE 3

Patch Thickness (mm)	$\sigma_{y\max}$ (kPa)
0·127	10490
0·254	6780
0·381	5128
0·508	4159
0·762	3040

Knowing the stress distribution in the patch it is possible to calculate the load carried by the patch. In this case it is of interest to note that increasing the thickness of the patch from 0·5 mm to 0·76 mm increases the load in the patch by only 9·6%.

Let us now examine the effect of a debond between the plate and the adhesive; the debond is assumed to occur only in the vicinity of the crack and has a width of 5·08 mm. For each patch configuration mentioned above the effect of the debond on the stress intensity factor and on the stresses in the patch was less than 0·1%. The major effect of the debond was to lower the τ_{zy} stresses in the adhesive at the crack. This effect can be seen in Figures 5, 6, 7 and 8. However, as can also be seen in these Figures, the shear stress at the edge of the debonded region is virtually unaffected by the existence of a debond.

These comments apply only to a relatively small debond along the crack; however, there is no physical reason to suppose that a debond does in fact exist, indeed as mentioned in reference [3] the presence of a debond around the crack in an actual experimental specimen has not yet been reported. Consequently if a debond does exist its width must be small. The theoretical existence of a debond is totally dependent upon the theoretically zero width of a crack and the resultant stress discontinuity, in the adhesive, across the crack. However, in practice the crack has a small but finite width so that this discontinuity will not occur. The shear stress in the adhesive will still be high in the vicinity of the crack and in the normal range of the working stresses the adhesive may go plastic. Indeed since Figures 5, 6, 7 and 8 show that the shear stress in the adhesive at the crack is of the same order of magnitude as the shear stresses at the edge of the patch the authors believe that, as discussed by Hart Smith[7], in the normal range of the working stresses the adhesive close to the ends of the patch and the adhesive directly over the crack may be behaving plastically, and that debonding may not occur.

As a result of this analysis, the authors believe that failure of a patched crack will primarily be determined by the same failure modes as reported in reference [7]. These are as follows. First, as a result of the adhesive going plastic the rate of increase of the stress intensity factor with load will be dramatically increased so that the applied load may cause K_1 to exceed K_{1c}, the fracture toughness of the plate. Second, the ultimate shear strain of the adhesive may be exceeded resulting in bond failure (this was the usual experimental failure mode reported by Hart Smith [7]). Finally, the peel stresses induced at the ends of the patches may cause failure, or the composite patch may itself fail.

---

7. L. J. Hart Smith — Analysis and design of advanced composite bonded joints, NASA CR-2218, August 1974.

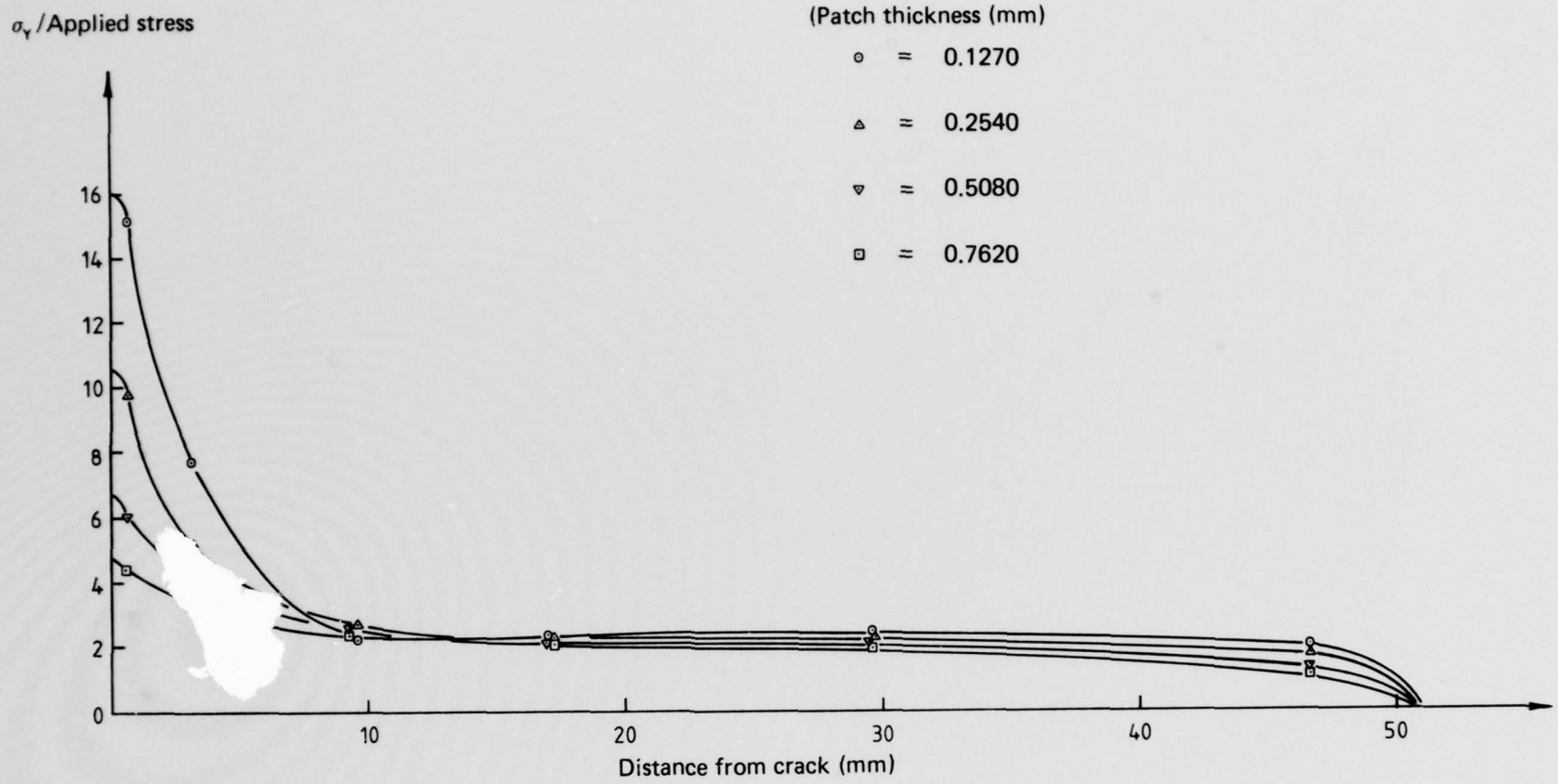

FIG. 9 VARIATION OF PATCH STRESS WITH DISTANCE FROM CRACK (Left hand side of patch)

APPENDIX I

Determination of the Stiffness Matrix for the Adhesive Element

From equation (3.6)

$$V_a = \frac{t_a}{2G_a}\iint [F_1(\Sigma_p \phi_p(u_o - u_s)_p)^2 + F_3(\Sigma_p \phi_p(v_o - v_s)_p)^2 + 2F_2(\Sigma_p \phi_p(u_o - u_s)_p)(\Sigma_q \phi_q(v_o - v_s)_q)]\, dxdy \quad \text{(i)}$$

The first row in the stiffness matrix is obtained by differentiating with respect to u_{si} (i.e. u_{sp} with $p = i$) which represents the value of u_s at the ith node. Differentiating we obtain

$$\frac{\partial V_a}{\partial u_{si}} = \frac{t_a}{G_a}\iint [F_1 \phi_i(\Sigma_p \phi_p(u_s - u_o)_p) + F_2\phi_i(\Sigma_q \phi_q(v_s - v_o))\, dxdy = \Sigma_n K_{1n}\lambda_n \quad \text{(ii)}$$

where λ_n is the nth term in the vector $\underset{\sim}{\lambda}$ as given by equation (3.9) and K_{1n} is the nth term in the first row of the stiffness matrix of the adhesive. Following the general technique the stiffness matrix K is found to be as shown in Table 1A.

Here, for the sake of convenience, we have written

$$<i, j> = \iint \phi_i\phi_j dxdy \quad \text{(iii)}$$

$$<i, m> = \iint \phi_i\phi_m dxdy \quad \text{(iv)}$$

$$<i, i> = \iint \phi^2_i dxdy \quad \text{(v)}$$

where the functions ϕ_i, ϕ_j and ϕ_m are as given by equation (3.5). Following this general technique the stiffness matrix $K^e{}_a$ is found to be as shown below:

$$K^e{}_a = (t_a/G_a)\begin{bmatrix}
F_1\langle i,i\rangle & F_2\langle i,i\rangle & -F_1\langle i,i\rangle & -F_2\langle i,i\rangle & F_1\langle i,j\rangle & F_2\langle i,j\rangle & -F_1\langle i,j\rangle & -F_2\langle i,j\rangle & F_1\langle i,m\rangle & F_2\langle i,m\rangle & -F_1\langle i,m\rangle & -F_2\langle i,m\rangle \\
F_2\langle i,i\rangle & F_3\langle i,i\rangle & -F_2\langle i,i\rangle & -F_3\langle i,i\rangle & F_2\langle i,j\rangle & F_3\langle i,j\rangle & -F_2\langle i,j\rangle & -F_3\langle i,j\rangle & F_2\langle i,m\rangle & F_3\langle i,m\rangle & -F_2\langle i,m\rangle & -F_3\langle i,m\rangle \\
-F_1\langle i,i\rangle & -F_2\langle i,i\rangle & F_1\langle i,i\rangle & F_2\langle i,i\rangle & -F_1\langle i,j\rangle & -F_2\langle i,j\rangle & F_1\langle i,j\rangle & F_2\langle i,j\rangle & -F_1\langle i,m\rangle & -F_2\langle i,m\rangle & F_1\langle i,m\rangle & F_2\langle i,m\rangle \\
-F_2\langle i,i\rangle & -F_3\langle i,i\rangle & F_2\langle i,i\rangle & F_3\langle i,i\rangle & -F_2\langle i,j\rangle & -F_3\langle i,j\rangle & F_2\langle i,j\rangle & F_3\langle i,j\rangle & -F_2\langle i,m\rangle & -F_3\langle i,m\rangle & F_2\langle i,m\rangle & F_3\langle i,m\rangle \\
F_1\langle i,j\rangle & F_2\langle i,j\rangle & -F_1\langle i,j\rangle & -F_2\langle i,j\rangle & F_1\langle j,j\rangle & F_2\langle j,j\rangle & -F_1\langle j,j\rangle & -F_2\langle j,j\rangle & F_1\langle j,m\rangle & F_2\langle j,m\rangle & -F_1\langle j,m\rangle & -F_2\langle j,m\rangle \\
F_2\langle i,j\rangle & F_3\langle i,j\rangle & -F_2\langle i,j\rangle & -F_3\langle i,j\rangle & F_2\langle j,j\rangle & F_3\langle j,j\rangle & -F_2\langle j,j\rangle & -F_3\langle j,j\rangle & F_2\langle j,m\rangle & F_3\langle j,m\rangle & -F_2\langle j,m\rangle & -F_3\langle j,m\rangle \\
-F_1\langle i,j\rangle & -F_2\langle i,j\rangle & F_1\langle i,j\rangle & F_2\langle i,j\rangle & -F_1\langle j,j\rangle & -F_2\langle j,j\rangle & F_1\langle j,j\rangle & F_2\langle j,j\rangle & -F_1\langle j,m\rangle & -F_2\langle j,m\rangle & F_1\langle j,m\rangle & F_2\langle j,m\rangle \\
-F_2\langle i,j\rangle & -F_3\langle i,j\rangle & F_2\langle i,j\rangle & F_3\langle i,j\rangle & -F_2\langle j,j\rangle & -F_3\langle j,j\rangle & F_2\langle j,j\rangle & F_3\langle j,j\rangle & -F_2\langle j,m\rangle & -F_3\langle j,m\rangle & F_2\langle j,m\rangle & F_3\langle j,m\rangle \\
F_1\langle i,m\rangle & F_2\langle i,m\rangle & -F_1\langle i,m\rangle & -F_2\langle i,m\rangle & F_1\langle j,m\rangle & F_2\langle j,m\rangle & -F_1\langle j,m\rangle & -F_2\langle j,m\rangle & F_1\langle m,m\rangle & F_2\langle m,m\rangle & -F_1\langle m,m\rangle & -F_2\langle m,m\rangle \\
F_2\langle i,m\rangle & F_3\langle i,m\rangle & -F_2\langle i,m\rangle & -F_3\langle i,m\rangle & F_2\langle j,m\rangle & F_3\langle j,m\rangle & -F_2\langle j,m\rangle & -F_3\langle j,m\rangle & F_2\langle m,m\rangle & F_3\langle m,m\rangle & -F_2\langle m,m\rangle & -F_3\langle m,m\rangle \\
-F_1\langle i,m\rangle & -F_2\langle i,m\rangle & F_1\langle i,m\rangle & F_2\langle i,m\rangle & -F_1\langle j,m\rangle & -F_2\langle j,m\rangle & F_1\langle j,m\rangle & F_2\langle j,m\rangle & -F_1\langle m,m\rangle & -F_2\langle m,m\rangle & F_1\langle m,m\rangle & F_2\langle m,m\rangle \\
-F_2\langle i,m\rangle & -F_3\langle i,m\rangle & F_2\langle i,m\rangle & F_3\langle i,m\rangle & -F_2\langle j,m\rangle & -F_3\langle j,m\rangle & F_2\langle j,m\rangle & F_3\langle j,m\rangle & -F_2\langle m,m\rangle & -F_3\langle m,m\rangle & F_2\langle m,m\rangle & F_3\langle m,m\rangle
\end{bmatrix}$$

APPENDIX II

Stiffness Matrix for Combined Patch-Adhesive Element

Define a vector $\delta(i)$, where i takes the values 1 to 12, such that $\delta(3) = 1$, $\delta(4) = 2$, $\delta(7) = 3$, $\delta(8) = 4$, $\delta(11) = 5$, $\delta(12) = 6$ and $\delta(i)$ is zero for all other values of i. Also define a vector $R(i)$ such that $R(i)$ is zero whenever $\delta(i)$ is zero and $R(i) = 1$ whenever $\delta(i)$ is not zero. Then if the stiffness matrix of the adhesive is denoted by K_a, and the stiffness matrix of the patch is denoted by K_p, the stiffness matrix of the patch-adhesive pair K is given by

$$K(i,j) = K_a(i,j) + R(i)R(j)K_p(\delta(i), \delta(j)) \tag{i}$$

where i and j take on the values 1 to 12.

DISTRIBUTION

	Copy No.
AUSTRALIA	
DEPARTMENT OF DEFENCE	
Central Office	
Chief Defence Scientist	1
Executive Controller, ADSS	2
Superintendent, Defence Science Administration	3
Defence Library	4
J.I.O.	5
Assistant Secretary, DISB	6–21
Aeronautical Research Laboratories	
Chief Superintendent	22
Superintendent, Structures Division	23
Divisional File, Structures Division	24
Authors: R. Jones	25
R. J. Callinan	26
Library	27
B. C. Hoskin	28
Materials Research Laboratories	
Library	29
Weapons Research Establishment	
Library	30
Central Studies Establishment	
Library	31
Engineering Development Establishment	
Library	32
RAN Research Laboratory	
Library	33
Air Force Office	
Aircraft Research and Development Unit	34
Air Force Scientific Adviser	35
Engineering (CAFTS) Library	36
D.Air Eng.	37
H.Q. Support Command (SENGSO)	38
Army Office	
Army Scientific Adviser	39
Royal Military College	40
US Army Standardisation Group	41
Navy Office	
Naval Scientific Adviser	42
DEPARTMENT OF PRODUCTIVITY	
Government Aircraft Factories	
Library	43

DEPARTMENT OF TRANSPORT

Director-General/Library		44
Airworthiness Group (Mr. R. Ferrari)		45

STATUTORY, STATE AUTHORITIES AND INDUSTRY

C.S.I.R.O., Central Library		46
C.S.I.R.O., Mechanical Engineering Division (Chief)		47
Qantas, Library		48
Trans Australia Airlines, Library		49
Ansett Airlines of Australia, Library		50
BHP Central Research Laboratories, NSW		51
BHP Melbourne Research Laboratories		52
Commonwealth Aircraft Corporation (Manager)		53
Commonwealth Aircraft Corporation (Manager of Engineering)		54
Hawker de Havilland Pty Ltd (Librarian) Bankstown		55
Hawker de Havilland Pty Ltd (Manager) Lidcombe		56

UNIVERSITIES AND COLLEGES

Adelaide	Barr Smith Library	57
	Professor of Mechanical Engineering	58
Australian National	Library	59
Flinders	Library	60
James Cook	Library	61
La Trobe	Library	62
Melbourne	Engineering Library	63
Monash	Library	64
Newcastle	Library	65
New England	Library	66
New South Wales	Physical Sciences Library	67
	Assoc. Professor R. W. Traill-Nash, Structural Engineering	68
Queensland	Library	69
Sydney	Professor G. A. Bird, Aeronautical Engineering	70
	Professor R. Wilson, Applied Mathematics	71
Tasmania	Engineering Library	72
Western Australia	Library	73
RMIT	Library	74

CANADA

Aluminium Laboratories Ltd, Library	75
CAARC Co-ordinator Structures	76
NRC, National Aeronautics Establishment, Library	77
NRC, Division of Mechanical Engineering (Dr. D. McPhail, Director)	78

UNIVERSITIES

McGill Library	79
Toronto Institute of Aerophysics	80

FRANCE

AGARD, Library	81
ONERA, Library	82
Service de Documentation, Technique de l'Aeronautique	83

GERMANY

ZLDI	84

Brooklyn	Library, Polytech Aeronautical Laboratories	172
California	Library, Guggenhein Aeronautical Laboratories	173
Spares		174–183